BNL-101389-2014-TECH
RHIC/DET/5;BNL-101389-2013-IR

Local shielding requirements for the STAR detector

A. Stevens

June 1992

Collider Accelerator Department
Brookhaven National Laboratory

U.S. Department of Energy
USDOE Office of Science (SC)

DISCLAIMER

BROOKHAVEN NATIONAL LABORATORY

June 1992 RHIC DETECTOR NOTE RHIC/DET Note 5

Local Shielding Requirements for the STAR Detector

Alan Stevens

Brookhaven National Laboratory
Upton, NY 11973

Local Shielding Requirements for the STAR Detector

I. Introduction

This note describes a series of calculations whose purpose was to estimate the radiation dose levels behind a shielded enclosure in the 6 o'clock hall. An enclosure "close to" the detector is required by the STAR collaboration in order to have access to electronics when the collider is running. As reported elsewhere[1], the thickness required for such an enclosure is determined by the possibility of nearby beam faults. For this reason, the vast majority of this note addresses radiation dose levels from "worst-case" faults as defined in the next section. The (very small) radiation levels from beam-beam and beam-gas interactions are briefly discussed at the end.

All the calculations were performed with the hadron cascade monte carlo program CASIM.[2,3] The quantity actually calculated by CASIM is the star density per interacting primary particle (SD) as a function of position in the enclosure material. This quantity, which is the number of interactions per unit volume per primary of all hadrons above the CASIM threshold of 0.3 GeV/c, is related to total dose by the following: Dose (rem/primary) = $2.25 \times 10^{-7} \cdot L \cdot SD$ where L is the (high energy) neutron interaction length in cm. and SD is in units of stars/cm^3primary. The calibration factor incorporates dose from particles below the CASIM threshold which are assumed to be in equilibrium with the hadrons transported by CASIM. Dose estimates obtained by this methodology agree well, i.e., typically within a factor of two, with measurements made at both FNAL[4] and the AGS[5] under controlled beam loss conditions.

II. Fault Simulation Assumptions

The policy at RHIC[6] is that the design of shielding enclosures should be of sufficient thickness to limit dose to a Radiation Worker in a high occupancy area to 0.5 rem in the event of a worst-case fault which is defined as loss of the entire beam on any magnet.[7] In actual practice, real faults will normally result in the vast majority of the beam being kicked on the internal dump. If a dump trigger or kicker should fail during fault conditions, most of the beam should interact on objects which define the aperture which include the internal dump, collimators, and high-beta quadrupoles (Q2 and Q3). Any rational fault model cannot, therefore, simulate the "loss of the entire beam on ANY magnet" definition so that some arbitrariness in defining the position of beam loss is required.

We have approximated a RHIC magnet by a coil/yoke cylinder of steel which

surrounds a 3.55 mm radially thick beam pipe.[8] If the cylinder (magnet) has a length L in the beam (Z) direction, then we define loss "on a magnet" as incident particles interacting uniformly along the length L at a depth of 1 mm into the beam pipe at the midplane azimuthal position. Uniformity in the Z direction is chosen simply because, in the absence of a fault model, no other choice is reasonable. Loss is forced on the magnet midplane because both many fault conditions (e.g. - a shorted coil in a dipole) will affect the bending plane orbit more than the vertical and because this choice gives somewhat higher radiation levels. The choice of 1mm depth comes from the following order-of-magnitude argument. In a linear machine, the divergence, x', in the transverse coordinate x is of order $\alpha \cdot x/\beta$ where α and β are the usual lattice parameters. If one pretends that the beam could blow up to a value of x equal to the vacuum pipe radius, then an x' is defined and a reasonable depth of interaction would be $L_{int} \cdot x'$ where L_{int} in the nuclear interaction length. In the insertion regions close to the experimental halls, the vacuum pipe radius, lattice functions, and interaction lengths all vary (the last because both protons and heavy ions are considered), but typical values for the depth of interaction obtained in this way range between .05 mm and 2 mm. Although the value of 1 mm was assumed in all cases for the results given below, a limited number number of calculations were performed forcing interactions at 0.1 mm depth and no difference (<20%) was observed.

III. Description of the Calculations

The approximation used for the magnets in the immediate vicinity of the 6 o'clock region is sketched in Fig. 1. Only one ring is included in the simulation whose axis is the beam axis (Z coordinate) in the hall. The outer boundaries of the magnets shown in Fig. 1 are the approximate radii of the yokes and no distinction is made between the coils and yokes both of which are taken to be steel. In all calculations magnetic fields (appropriate for $\beta^* = 6$m) are assumed within the aperture shown. No fringe fields are included and the "return fields" in the yokes are ignored.

Fig. 2 shows the two-dimensional approximation of the geometry in the hall region. In this figure Z=0 marks the beginning of the hall and corresponds to Z ~ 26.5m in Fig. 1. The only materials considered to be present in the hall are the beam pipe, the return yoke and end cap(s) of the STAR solenoid[9], and the enclosure itself. The latter is assumed to be heavy concrete[10] whose front wall and side wall begin at R = 4.4m and Z = 2.75m respectively. Both walls are 1.20m thick (~4 ft.) which preliminary calculations showed to be approximately the required thickness. The dashed lines on the enclosure and magnet indicate that most calculations were terminated at Z ~ 9m, which a subset of calculations showed to be sufficient.

Two-dimensional calculations are required because of the prohibitive computer time required to obtain good statistical accuracy in a full three-dimensional geometry. The meaning of "two-dimensional" in the CASIM context is that the material and star binning assume azimuthal symmetry. However, the tracking is performed in three dimensions which allows approximate "corrections" to be made for effects which break this symmetry. In this

case, the symmetry is broken by the magnetic fields in the insertion region magnets. These fields cause star density enhancement in the horizontal plane relative to the azimuthally averaged star density. To correct the averaged values, the azimuth was divided into four segments and a count was made of the total "left-right" stars versus "up-down" stars in the shielding enclosure. This count was used to modify (increase) the average value of the star density in the two-dimensional results presented in the next section.

To compare with the two-dimensional results, and to obtain information inherently not ascertainable with a two-dimensional approximation, a limited number of calculations were made in a full three-dimensional geometry. In this geometry the enclosure is composed of three rectangular slabs; a front wall, side wall, and roof. The front wall begins at Z = 2.75m, is 1.20m thick in the lateral (X) direction and extends vertically from Y = 0 to Y = 3.05m where Y = 0 marks the floor level in the 6 o'clock hall. The side wall abuts the front wall, beginning at X = 5.6m and Z = 2.75m with a Z thickness of 1.20m and the same vertical extent as the front wall. These are overlaid with a roof. Fig. 3 shows an X,Y section at Z = 8m (see Fig. 2). The roof thickness shown in Fig. 3 is 90 cm. (~3 ft.) although calculations were made for both 90 cm. and 120 cm. thick roofs. As mentioned above, this geometry suffers from poor statistical precision given finite computing resources. Although not shown in Fig. 3, an X-reflected enclosure was included in the star-binning routine and, similar to the azimuthal correction in the two-dimensional geometry, a count was maintained of the total enclosure stars on the ring-inside side (where the enclosure actually will exist) versus the ring outside. The correction in this case measures the charge asymmetry of secondaries.

Calculations were made only for protons at 250 GeV/c and Au ions at 100 GeV/u. Stars were accumulated in bin sizes whose linear dimensions ranged between 12 and 30.5 cm. In all cases dose estimates are obtained from the star densities accumulated in the bins closest to the enclosure interior with small corrections applied such that the point of evaluation corresponds to a wall thickness of exactly 4 ft. (or 3 ft. in one of the roofs considered). This essentially assumes that a person can be immediately behind one of the walls. Combining the design intensities of 5.7×10^{12} protons/ring or 5.7×10^{10} Au ions per ring with the star density to dose conversion described in section I gives a 500 mrem fault dose level which corresponds to 1.23×10^{-8} stars/cm^{3}proton or 1.23×10^{-6} stars/cm^{3}Au ion.

IV. Results

(A): Two-dimensional Geometry

Fig. 4 shows the corrected[11] star density vs. distance (R) on the inside of the side wall (see Fig. 2) for loss on the closest magnet, DX. The errors shown in this figure (and all subsequent figures) are determined from a few (typically 3 to 5) computer runs with differing random number seeds. In order to avoid the awkward cases where the 1 sigma estimator from only a few trials gives an anomolously low value, a 10% lower limit to the error bars shown has been assigned.

Fig. 5 shows the corresponding star densities along the back of the front wall. The Z dependence is relatively small. We take the maximum star density averaged over 1.2m (5 Z bins in Fig. 5) as the measure of the radiation level on this enclosure boundary. Both this quantity and the star density in the first radial bin (closest to the beam axis) are shown as a function of source loss position in Fig. 6 for 250 GeV/c protons. In addition to loss on the magnets indicated, Fig. 6 shows a loss source on the "beam pipe" which was obtained by forcing interactions over a 3m length of the beam pipe immediately inside the hall. Although this source position is closer to the enclosure than DX, the radiation dose level is much reduced because forward energy can easily escape both sides (radially) of the beam pipe. Fig. 6 verifies[12] that the closest magnet, DX, is the worst source location for a fault and only this location was considered in the three-dimensional calculations. In order to determine the effect of the transverse starting distance of the enclosure, a limited number of calculations were performed with R = 5.5m instead of 4.4m. The results verified that both the side and front wall star densities exhibit a $1/R^2$ dependence.

(B): Three-dimensional Geometry

The locations in the three-dimensional geometry which can be directly compared to the two-dimensional results are the backs of the front and side walls at the high vertical (Y) coordinate. We show in Table I below this comparison where the two-dimensional results have been multiplied by 1.14. This factor is the ring-inside vs. ring-outside factor mentioned above obtained from the three-dimensional results; the fact that the star density is higher on the ring-inside stems from the fact that the magnetic field in DX bends positive secondaries toward the ring-inside at 6 o'clock.

Table I

Maximum Star Densities in Two and Three Dimensions with Source on DX

	2D Au (Stars/cm^3•ion X10^{-6})	3D Au (Stars/cm^3•ion X10^{-6})	2D Proton (Stars/cm^3•p X10^{-8})	3D Proton (Stars/cm^3•p X10^{-8})
Side Wall	1.46 ± 0.32	2.20 ± 1.54	1.70 ± 0.33	1.90 ± 0.73
Front Wall	1.47 ± 0.15	1.10 ± 0.20	1.65 ± 0.17	1.55 ± 0.29

Although the statistical errors in the three-dimensional calculations are generally large, the results for these "hot-spots" are in agreement with the charge-asymmetry corrected two-dimensional results which will be regarded as definitive.

As mentioned above, three-dimensional calculations were performed with both 3 ft. and 4 ft. roof thicknesses. In order to achieve (barely) adequate statistical precision here, the star density on the bottom of the roof was averaged over 5m in the Z (beam) direction and the results increased by the ratio of the 1.2m average to the 5m average obtained from the front wall two-dimensional calculations. With this correction, the star density on the bottom of the roof immediately in back of the front wall is shown in Table II.

Table II

Star Densities on Roof Underside Closest to Beam Axis with Source on DX

	3 ft. roof (Stars/cm^3•incident)	4 ft. roof (Stars/cm^3•incident)
Au	$1.39 \pm 0.53 \times 10^{-6}$	$7.28 \pm 4.05 \times 10^{-7}$
Protons	$1.01 \pm 0.30 \times 10^{-8}$	$8.01 \pm 3.48 \times 10^{-9}$

At one meter further away from the beam line, X = 6.6m, the star density on the roof underside is decreased from the values shown in Table II by a factor of about 3.[13] A similar factor is obtained when comparing the side or front wall star densities at the floor level (Y = 0) with the highest Y values shown in Table I.

(C): Shielding Recommendations and Caveats

The worst-case fault levels in Table I for the geometry considered exceeds the 500 mrem value ($1.23 \times 10^{-6/-8}$ stars/cm^3•ion/proton) by a small amount. Since the front and side wall star densities have been verified to decrease by $1/R^2$, beginning the enclosure shown at 5.2m from beam axis instead of 4.4m is sufficient. Alternatively, the enclosure could have its thickness increased by six inches of heavy concrete.[14]

The star density values obtained for the three ft. heavy concrete roof are consistent with the required level.

Both the side wall and roof thicknesses may be decreased with distance from the beam line. We make a conservative (e.g., see Fig. 4) recommendation that both be allowed to decrease by 1 ft. of heavy concrete equivalent[14] every two meters until a **minimum** thickness of two ft. of heavy concrete equivalent is reached. Thus, if the front wall ends at 6.4m (5.2m + 1.2m), the side wall could be decreased from 4 ft. to 3 ft. at X = 8.4m and to 2 ft. at X ≥ 10.4m, and the roof thickness could be decreased from 3 ft. to 2 ft. for X ≥ 8.4m. Some consideration is being given to increasing the vertical extent of the enclosure interior (see Fig. 3) to a height greater than the return yoke.[15] If this should be the case, there would be no direct radiation source "shining down" on the roof, but skyshine from low

energy neutrons, which CASIM does not properly take into account in these geometries would still exist, so it is recommended that the minimum roof thickness of 2 ft. of heavy concrete still be required.

Two caveats must be mentioned. The first is that new regulatory requirements in the DOE RadCom Manual raise the quality factor for neutrons by a factor of two for new facilities.[16] This would increase the CASIM star density to rem conversion by nearly this factor which implies an additional thickness of almost 1 ft. of heavy concrete at the same transverse distance. However, it is not clear that RHIC is a "new facility" as regards this requirement or that the criteria could not be revised to allow 1 rem for worst-case faults if the quality factor change is required to be considered.[6] A second caveat concerns the beam intensity. If the beam intensity increases beyond the design intensity, additional shielding must be added. Leaving space between the horizontal extent of the yoke and the beginning of the enclosure, as has been assumed here, would allow addtional shielding to be added between the enclosure and the detector should that be required.

V. Beam-beam and Beam-gas Radiation Levels

For completeness, an estimate of beam-beam and beam-gas radiation dose levels are given here based on previous work.[1] For Au on Au at a luminosity of 2×10^{26} cm^2/sec, the dose at a distance R from the beam has been estimated to be $0.61 \cdot \exp(-S/.195)/R^2$ mrem/hr where S is the shielding thickness in meters of steel equivalent and R is in meters. In this case, assuming a 4 ft. heavy concrete enclosure beginning at 5.2m, R ~ 6.4m and S = 0.64m which gives a dose rate of 5.5×10^{-4} mrem/hr.

For an estimate of the beam-gas dose rate, we use the "beam pipe" result of 1.6×10^{-7} stars/cm$^3 \cdot$Au ion (see Fig. 6 for the proton equivalent), which has approximately the correct geometry, coupled with the beam-gas interaction rate estimate of 800 Hz.[17] and the 5.2m position assumption. This gives[18] 2.3×10^{-3} mrem/hr.

VI. Summary

Worst-case fault conditions are defined as the loss of the entire RHIC design intensity of 5.7×10^{12} protons or 5.7×10^{10} Au ions at full energy on a single magnet. If such a loss were to occur on the magnet closest to the 6 o'clock hall, DX, an enclosure whose front and side walls are 4 ft. thick heavy concrete and which begins at 5.2m from the beam axis is required to limit the dose behind this enclosure to 500 mrem. The enclosure roof is required to be 3 ft. thick if the enclosure height is below the STAR magnet return yoke. The thickness of both the side wall and roof may be slowly reduced at larger distances from the beam axis as described in the text. Additional shielding and/or distance from the beam axis will be required if the beam intensity is increased and may be required if the neutron quality factor is increased without a concomitant increase in the allowable fault dose.

Radiation dose rates from beam-beam and beam-gas reactions behind this enclosure are negligible.

References/Footnotes

1. M. Fatyga and B. Moskowitz, "Fourth Workshop on Experiments and Detectors for a Relativistic Heavy Ion Collider," p. 254, BNL 52262 (1990).

2. A. Van Ginneken, "CASIM; Program to Simulate Hadron Cascades in Bulk Matter," Fermilab FN-272 (1975).

3. A.J. Stevens, "Improvements in CASIM; Comparison with Data," AGS/AD/Tech. Note No. 296 (1988). See also A.J. Stevens, "Maximum Energy Deposition Densities in the Internal Dump," AD/RHIC/RD-41 (1992). The last reference describes changes to CASIM to propagate fragments resulting from heavy ion collisions.

4. J.D. Cossairt, et. al.,"Absorbed Dose Measurements at an 800 GeV Proton Accelerator; Comparison with Monte Carlo Calculations," Nucl. Instr. & Meth. A238, p.504 (1985).

5. Using the calibration factor given in the text, a deep penetration shielding measurement in the D-line of the AGS of 126 mrem/hr compares to a CASIM prediction of 65 ± 19 mrem/hr. Details of this comparison are given in a memorandum from A.J. Stevens to D. Beavis dated 12/4/91. Again using this calibration for the transverse measurement reported in Ref. 3 predicts 60 ± 5 mrem/hr compared to a measured 48 ± 11 mrem/hr.

6. Draft version of section 3.9.2 of the RHIC Safety Analysis Document dated 06/09/92. It should be noted that the current version of this policy document assumes the same quality factor for neutrons as the CASIM star density to dose calibration constant.

7. Any object of sufficient thickness (several interaction lengths) would qualify as a "magnet."

8. This thickness is about twice the actual steel beam pipe thickness and is therefore treated as steel (Fe) with half the density - 3.9 g/cc. The beam pipe is treated in this manner to reduce the probability of "stepping over" the pipe during transport in the Monte Carlo.

9. The magnetic field of the solenoid is not considered.

10. Heavy concrete is considered to be a material with $Z = 18$, $A = 38$, and density = 3.6 g/cc.

11. The bending plane enhancement is approximately 22%. However, the total enhancement relative to an approximation which ignores the magnetic field in DX is a factor of 2. The azimuthally averaged star density increases when the field is included

because (some) charged secondaries do not escape down the vacuum pipe as they can in a field free region.

12. Results similar to those in Fig. 6 were obtained for an Au beam interacting on D0, DX, and the "beam pipe."

13. The error on this factor is considerable. The factor may be as low as 2 or as high as 4.5.

14. Both front and side walls show a decreasing star density with depth consistent with the "usual" CASIM values for transverse attentuation. For heavy concrete, the attenuation length is 40.8 cm. Equivalent attenuation lengths for other commonly used shielding materials are 50.2 cm. for light concrete (ρ = 2.4 g/cm^3) and 21.4 cm. for steel (ρ = 7.8 g/cm^3). The inner two ft. of the enclosure walls must, however, be composed of concrete or other similarly hydrogenous materials.

15. J. Mills, private communication.

16. S. Musolino, private communication.

17. S. White, "Beam-Gas Backgrounds," RHIC/DET Note 1 (1991). This assumes a vacuum of 10^{-9} Torr in the intersection region and includes both beams.

18. In this case, the star density of 1.6 X 10^{-7} stars/cm^3•ion times the CASIM conversion constant is 1.14 X 10^{-9} mrem per interacting Au ion. This estimate, whose underlying physics is Au ions interacting with Fe nuclei, should in fact overestimate the beam-gas dose rate because the gas composition is dominated by light nuclei such as helium. Likewise the 3m loss length assumption should in principle be modified to 10m for beam-gas, so the dose rate in the text should be regarded as an upper limit.

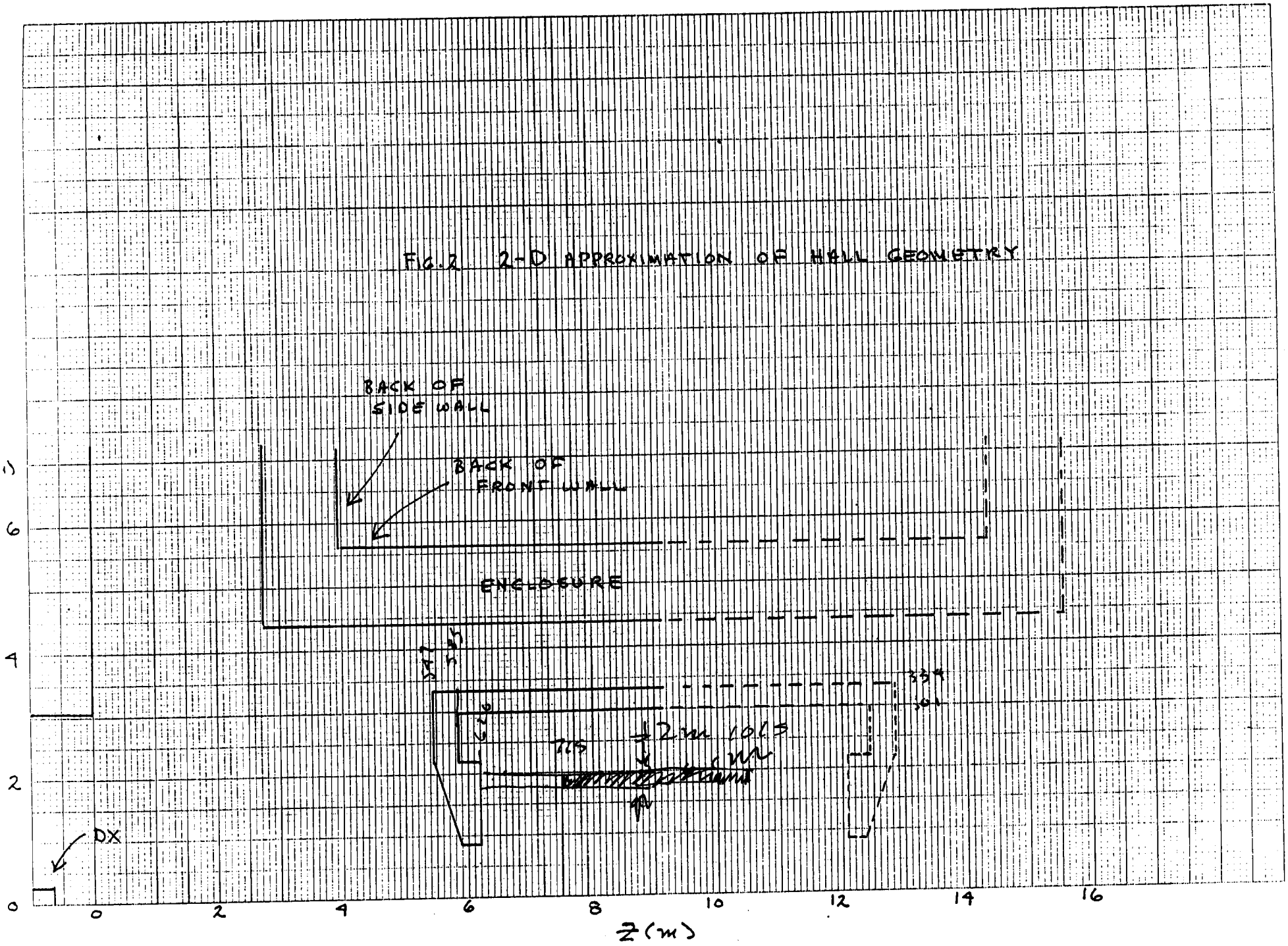

FIG. 2 2-D APPROXIMATION OF HALL GEOMETRY

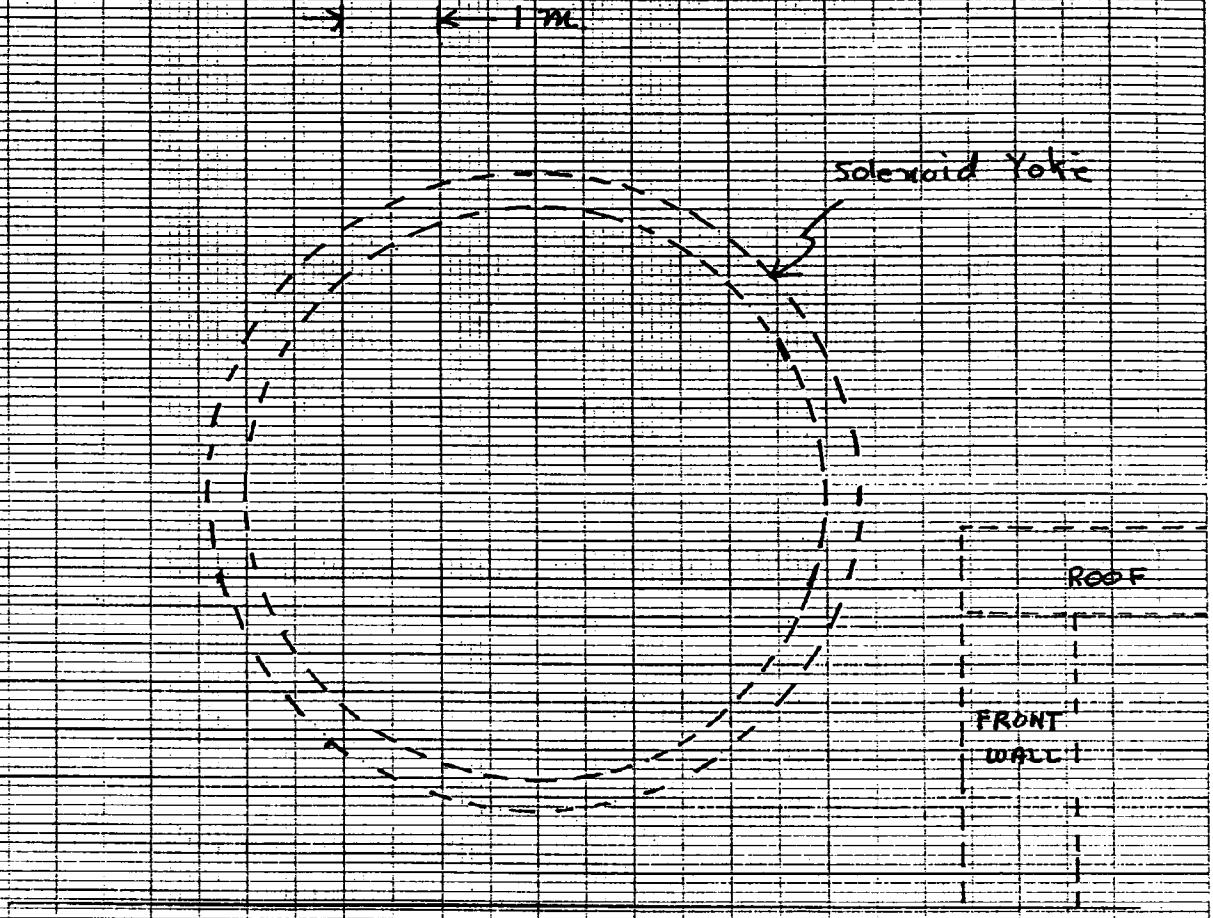

FIG. 3. X,Y CROSS-SECTION AT CONSTANT Z ILLUSTRATING 3-D GEOMETRY

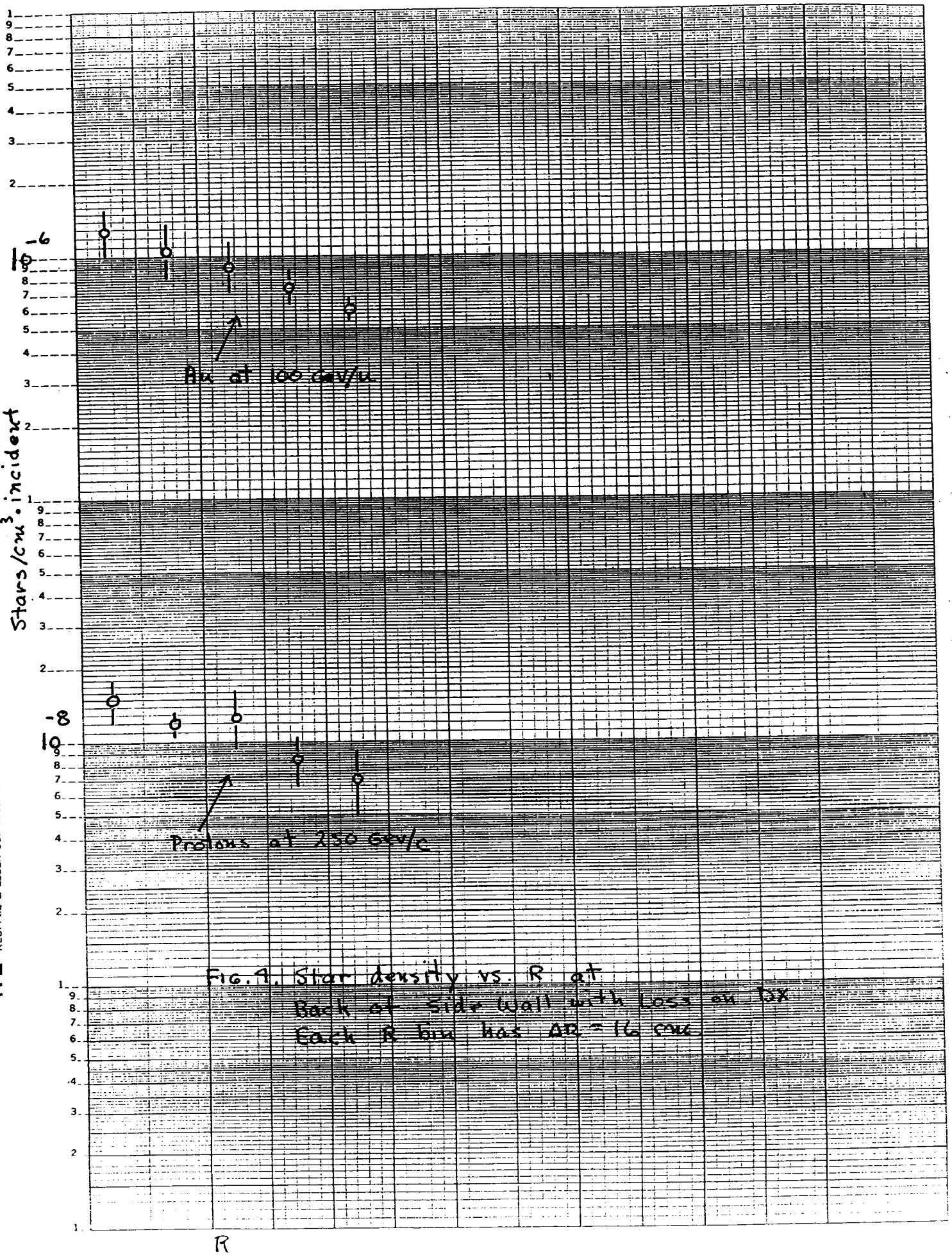

Fig. 7. Star density vs. R at Back of side wall with Loss on Dx
Each R bin has ΔR = 16 cm

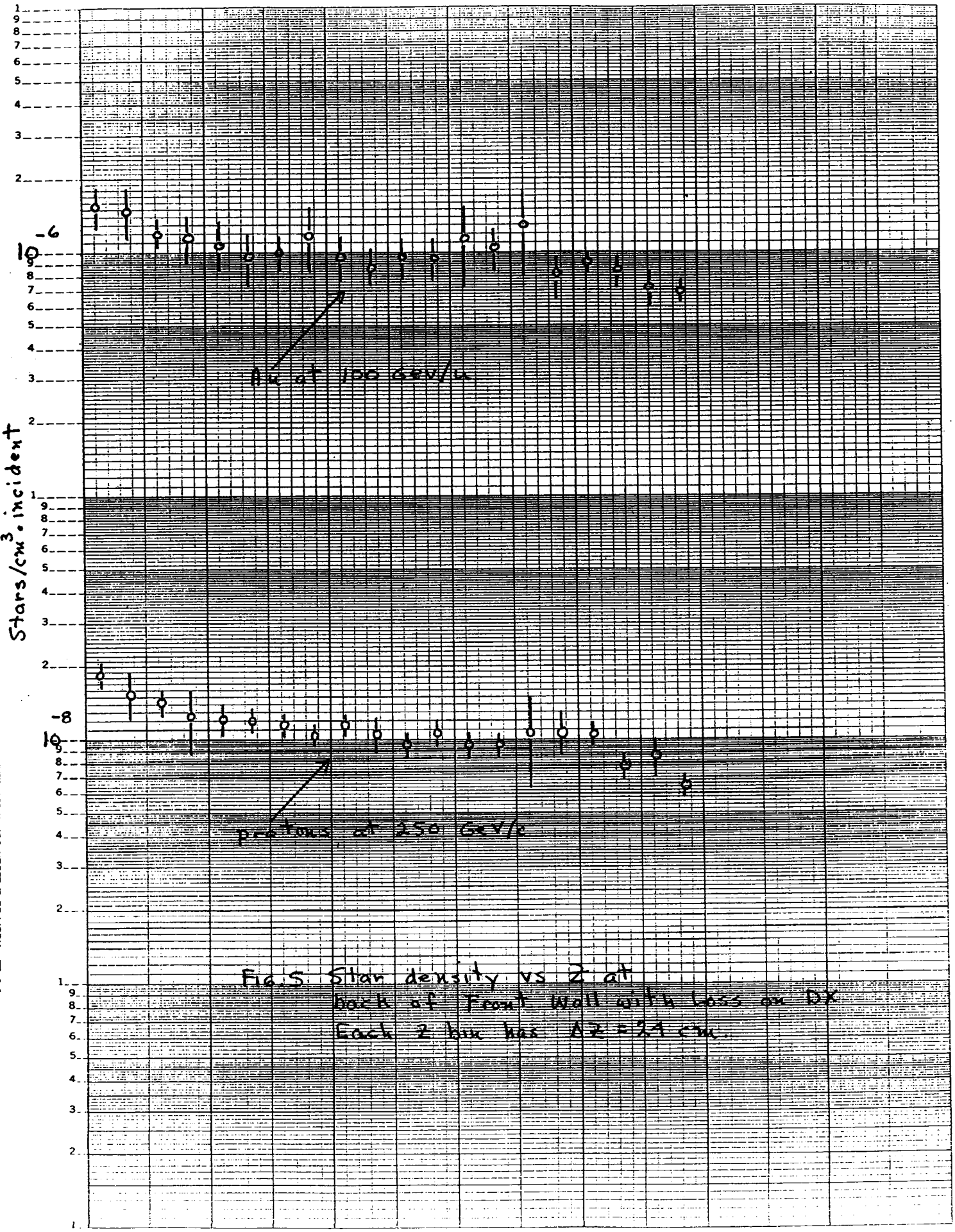

Fig. 5 Star density vs Z at back of front wall with loss on DX. Each 2 bin has ΔZ = 2.1 cm.

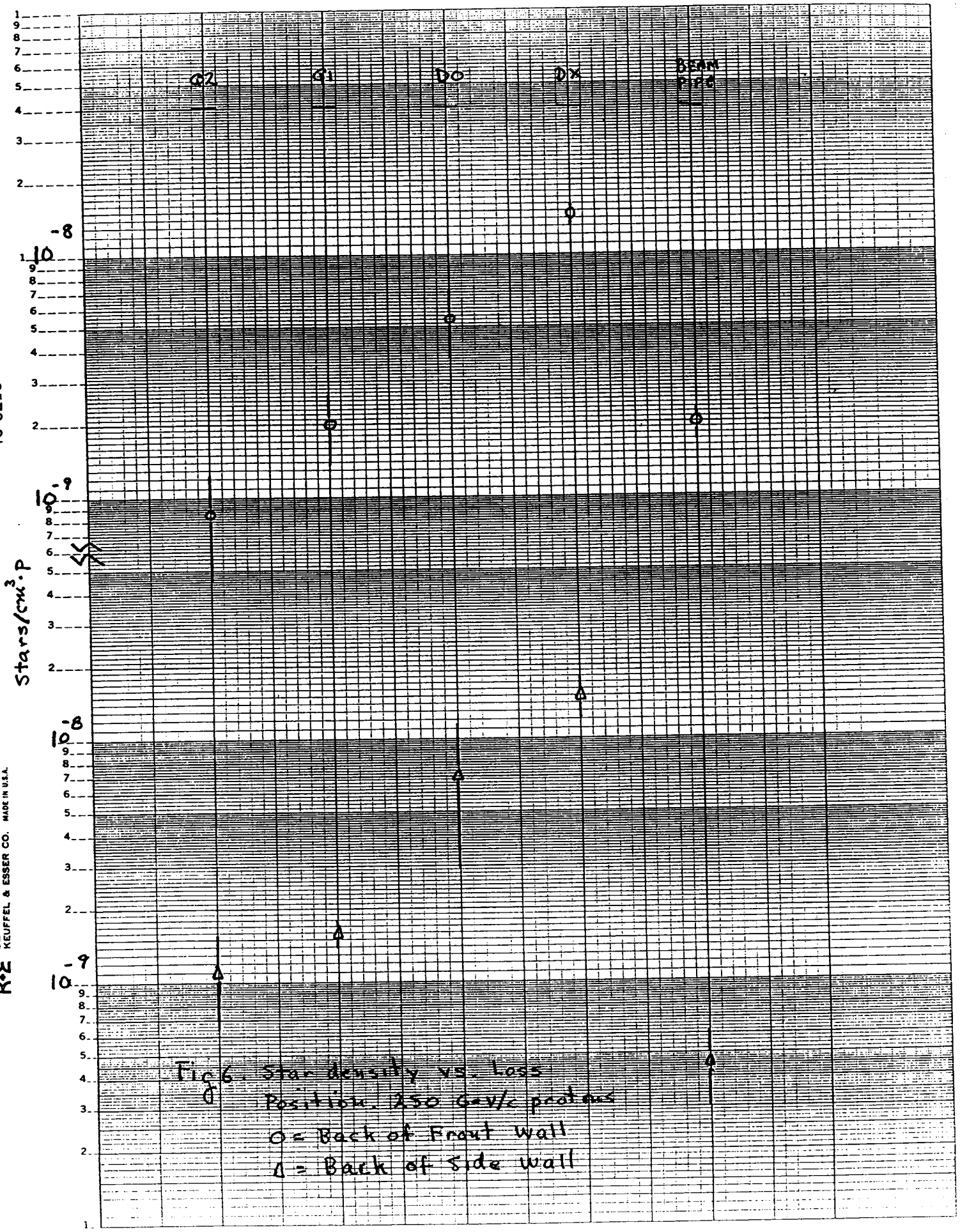

Fig 6. Star density vs. Loss Position. 250 Gev/c protons
○ = Back of Front Wall
△ = Back of Side Wall